Article

Quasifree Photoionization under the Reaction Microscope

Sven Grundmann [1], Florian Trinter [1,2], Yong-Kang Fang [3], Kilian Fehre [1], Nico Strenger [1], Andreas Pier [1], Leon Kaiser [1], Max Kircher [1], Liang-You Peng [3], Till Jahnke [4], Reinhard Dörner [1] and Markus S. Schöffler [1,*]

[1] Institut für Kernphysik, Goethe-Universität, Max-von-Laue-Straße 1, 60438 Frankfurt, Germany;
    grundmann@atom.uni-frankfurt.de (S.G.); trinter@atom.uni-frankfurt.de (F.T.);
    fehre@atom.uni-frankfurt.de (K.F.); strenger@atom.uni-frankfurt.de (N.S.); pier@atom.uni-frankfurt.de (A.P.);
    kaiser@atom.uni-frankfurt.de (L.K.); kircher@atom.uni-frankfurt.de (M.K.);
    doerner@atom.uni-frankfurt.de (R.D.)
[2] Molecular Physics, Fritz-Haber-Institut der Max–Planck–Gesellschaft, Faradayweg 4-6, 14195 Berlin, Germany
[3] State Key Laboratory for Mesoscopic Physics and Frontiers Science Center for Nano-Optoelectronics,
    School of Physics, Peking University, Beijing 100871, China; yongkangfang@pku.edu.cn (Y.-K.F.);
    liangyou.peng@pku.edu.cn (L.-Y.P.)
[4] European XFEL, Holzkoppel 4, 22869 Schenefeld, Germany; jahnke@atom.uni-frankfurt.de
[*] Correspondence: schoeffler@atom.uni-frankfurt.de

Abstract: We experimentally investigated the quasifree mechanism (QFM) in one-photon double ionization of He and H_2 at 800 eV photon energy and circular polarization with a COLTRIMS reaction microscope. Our work provides new insight into this elusive photoionization mechanism that was predicted by Miron Amusia more than four decades ago. We found the distinct four-fold symmetry in the angular emission pattern of QFM electrons from H_2 double ionization that has previously only been observed for He. Furthermore, we provide experimental evidence that the photon momentum is not imparted onto the center of mass in quasifree photoionization, which is in contrast to the situation in single ionization and in double ionization mediated by the shake-off and knock-out mechanisms. This finding is substantiated by numerical results obtained by solving the system's full-dimensional time-dependent Schrödinger equation beyond the dipole approximation.

Keywords: two-electron systems; one-photon double ionization; many-electron correlation

1. Introduction

The quasifree mechanism (QFM) is a special case of photo-double ionization (PDI) that was predicted by M. Amusia et al. in 1975 [1]. The name of the process originates from the idea that the photon interacts with a quasifree electron pair without involvement of the nucleus. The kinematic profile of QFM is characterized by electrons being emitted back-to-back with equal kinetic energy, which leave the nucleus with close-to-zero recoil momentum [2,3]. The interaction between photons and atoms is generally dominated by electric-dipole contributions, but the QFM profile is forbidden in a dipole transition due to angular momentum and parity conservation [4]. Hence, QFM facilitates double ionization by means of a pure electric-quadrupole transition. As QFM ejects two electrons only from the small part of the initial-state two-electron wave function where both electrons are spatially close together [5,6], its transition amplitude is extremely small and experimental investigations of QFM are challenging [7]. However, nearly four decades after the prediction, the existence of the quasifree mechanism was finally experimentally confirmed by Schöffler et al. in 2013 through the observation of doubly charged helium nuclei with close-to-zero momentum [8]. Note that this signature of QFM is similar to what is found for double ionization by Compton scattering which becomes the dominant double-ionization channel at high photon energies [9–11].

The recently renewed interest in nondipole photoionization in the one-photon and strong-field ionization regimes (see, e.g., Refs. [12–17]) encouraged further experimental

and theoretical investigations of QFM. In 2018, electrons emitted back-to-back with equal energy were observed for helium PDI at 1100 eV photon energy [18]. This work displayed the angular emission pattern of electrons originating from a pure quadrupole transition. Two years later, QFM was confirmed for H_2 PDI at 800 eV photon energy and it was shown how the QFM cross section relates to the initial spatial probability density at the two-electron cusp, which is the point where both electrons coalesce [19]. In the present work, we examine once again the experimental data used in Refs. [18,19] to continue the investigation of QFM. First, we will show that the angular distribution of QFM electrons originating from H_2 PDI displays the same four-fold symmetry that was already observed for He PDI. Furthermore, second, we will provide evidence for the assumption that the photon momentum is not imparted onto the center of mass in quasifree photoionization. The latter finding is supported by numerical results from solving the full-dimensional time-dependent Schrödinger Equation (TDSE) beyond the dipole approximation.

2. Methods

The two experiments reported here have been performed at beamline P04 at the PETRA III synchrotron (DESY, Hamburg, Germany [20]) using circularly polarized light at 800 eV photon energy. We employed a cold target recoil ion momentum spectroscopy (COLTRIMS) reaction microscope [21–23] and intersected a supersonic gas jet of He or H_2 with the photon beam at a right angle. Due to the supersonic expansion, the H_2 were in their vibrational ground state. The charged reaction fragments were projected by an electric field and guided by a magnetic field to two time- and position-sensitive detectors with delay-line position readout [24,25]. The initial momenta after PDI were retrieved from the particles' times-of-flight and positions of impact. The concept of a COLTRIMS reaction microscope is illustrated in Figure 1. The experimental results reported in the present work were obtained from the same experimental runs as Refs. [18,19], where further experimental details can be found.
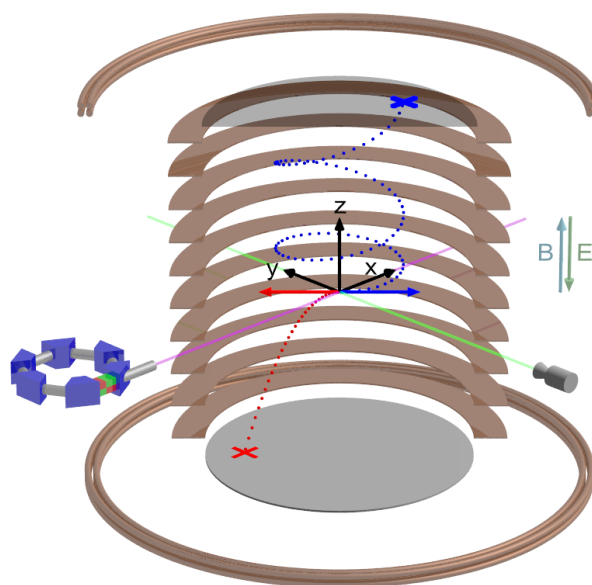

Figure 1. Concept of cold target recoil ion momentum spectroscopy (COLTRIMS). A supersonic jet (green) of a target gas is crossed with synchrotron light (violet) at a right angle. A homogeneous electric field *E*, generated by a spectrometer (copper plates), and a homogeneous magnetic field *B*, created by a Helmholtz pair (copper tubes), guide the charged reaction fragments (red trajectory: ion, blue trajectory: electron) towards time- and position-sensitive detectors. The initial three-dimensional momentum vector of each reaction fragment (blue and red arrows) was calculated from the time-of-flight and the position of impact on the detectors (marked with a blue and a red cross).

The two-electron nondipole TDSE code used here was developed based on our previous dipole code for helium, which has been successfully applied in a series of studies on the two-photon double ionization of helium [26–28]. The form of the Hamiltonian with the nondipole corrections and the chosen parameters in the calculations can be found in Ref. [29]. After the end of the light pulse, the two-electron wave function was further propagated freely for a time of 10 a.u. Then, it was projected onto the uncorrelated symmetrical product of two single-electron scattering states to obtain the joint momentum distribution of the two ejected electrons $P(k_1, k_2)$. The momentum spectrum of the ion $P(Q)$ could then be obtained from $P(k_1, k_2)$ by momentum conservation: $P(Q) = \int P(k_1, k_{\text{photon}} - k_1 - Q)dk_1$. For the case of the dipole approximation, k_{photon} was set to 0. In the calculations, a linearly polarized light pulse along the z axis was adopted, with its propagation direction in the x axis. Therefore, the momentum spectrum of the ion in the propagation direction of the light pulse was given by $P(Q_x) = \iint dQ_z dQ_y P(Q)$. For the distribution of $P(Q)$ in the PDI of helium, previous studies showed that the majority of the events are located close to the surface of a sphere in the momentum space with a radius of $p_{\text{single}} = \sqrt{\omega - I_p}$, where ω and I_p, respectively, represent the photon energy and ionization potential of helium. Such a behavior is closely related to the shake-off (SO) and the electron knock-out mechanism [8]. In order to show the effect of the QFM mechanism, we used a similar method as that in Ref. [8]. The integral interval in the light polarization direction of Q_z was limited from $-p_{\text{single}}/4$ to $p_{\text{single}}/4$. Furthermore, the integral interval of Q_y was limited by $|Q_y| \leq p_{\text{single}}/2$.

3. Results

3.1. Separating a Pure Quadrupole Contribution to Photo-Double Ionization

In quasifree photoionization, the photon is absorbed by the electron pair and the nucleus is only a spectator that receives no recoil momentum. By means of momentum and energy conservation, the ejection of two electrons back-to-back with equal energy is a strict consequence of a vanishing recoil momentum, if one neglects the photon momentum. For a dipole transition, this kinematic profile is forbidden for PDI of He and H_2, whose ground-state wave functions both have the same ^1S symmetry [4,30]. Hence, the QFM is a pure quadrupole contribution to PDI and it can be isolated particularly clearly in a differential cross section that shows the double-ionization yield as a function of the electron energy sharing $\varepsilon = E_{e1}/(E_{e1} + E_{e2})$ and the angle enclosed by the two electron momentum vectors $\vartheta_{12} = \cos^{-1}[p_{e1} \cdot p_{e2}/(|p_{e1}| \times |p_{e2}|)]$ (electron mutual angle). This is done in Figure 2 where we show the measured yield from the double ionization of H_2 (A,B) and He (D,E) at 800 eV photon energy as a function of ε and ϑ_{12}. Panels A and D show the full range of the two variables, but panels B and E show only the region indicated by the dashed black lines in A and D. A comparison between panels A and D points out a strong resemblance in the electron emission patterns of H_2 and He double ionization, as expected from the similarities in the electronic ground states. A distinctive difference can be seen around equal energy sharing ($\varepsilon = 0.5$) and back-to-back emission ($\cos \vartheta_{12} = -1$) where there appears to be a noticeable signal in panel A, corresponding to QFM, but apparently a node in panel D. Panels C and D highlight this relevant region of the cross section. While the QFM is evident for H_2, a logarithmic-scale display is required in panel D to make the weak relative contribution of QFM to the total double-ionization cross section of helium visible at all (see Ref. [19] for further discussions on this finding).
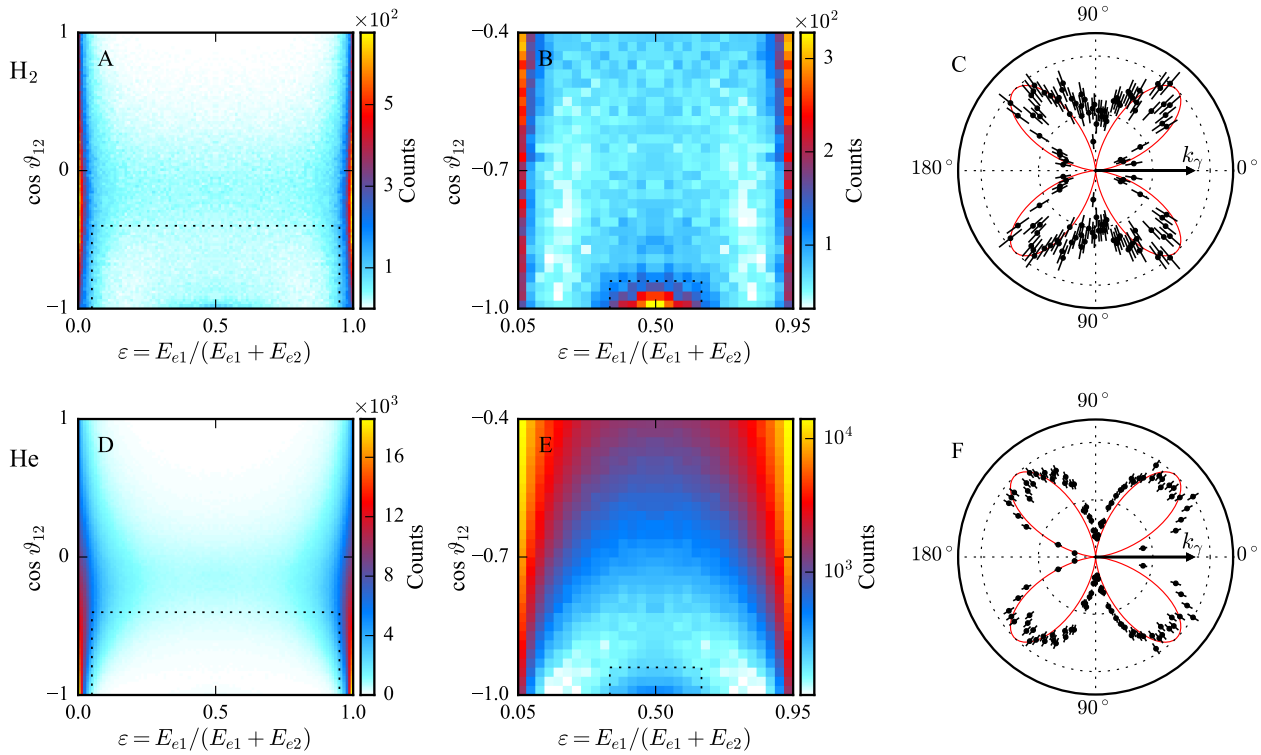
Figure 2. Measured electron distributions of H_2 double ionization (**A**–**C**) and He double ionization (**D**–**F**) by a single 800 eV circularly polarized photon. (**A**,**D**) Measured electron yield as a function of the electron energy sharing ε and the electron mutual angle ϑ_{12}. (**B**,**E**) Detailed section from panels A and D as indicated by the dashed black lines therein. Note the logarithmic-scale display in panel E. Contributions around $\varepsilon = 0.5$ and $\cos\vartheta_{12} = -1$ correspond to the QFM electrons. (**C**,**F**) Angular distributions of QFM electrons as a function of the polar angle enclosed by the electron momentum vector and the light propagation direction. The shown data are limited to $0.35 < \varepsilon < 0.65$ and $\vartheta_{12} > 160°$, as indicated by the dashed black lines in panels B and E. For this selection, the dipole contribution to photoionization vanishes. The red lines represent $|Y_{21}|^2$ and are normalized to the data points.

To highlight the quadrupole nature of QFM, we selected a subset of our data limited to $0.35 < \varepsilon < 0.65$ and $\vartheta_{12} > 160°$, as indicated by the dashed black lines in Figures 2B,E, and present in Figures 2C,F—the measured electron yield as a function of the angle ϑ_γ, which is enclosed by the electron momentum vector and the light propagation direction. The angular-momentum transfer is an important physical difference between dipole and quadrupole transitions. By definition, a dipole transition transfers one unit of angular momentum to the two-electron final state due to the photon spin, while two units of angular momentum are available in a quadrupole transition. The angular momentum of the outgoing electron wave becomes observable in the angular distribution of the electron. The red lines in Figures 2C,F represent the square of the spherical harmonic for $\ell = 2$ and $m = 1$, $|Y_{21}|^2 \propto \cos^2\vartheta_\gamma \times \sin^2\vartheta_\gamma$, which describes the final-state angular distribution of electrons that result from a pure electric-quadrupole transition from any initial *s*-subshell. Here, we have chosen the photon propagation direction $\hat{\boldsymbol{k}}_\gamma$ as the quantization axis. The photon spin vector is (anti-)parallel to $\hat{\boldsymbol{k}}_\gamma$ and we get $\Delta\ell = 1$ and $\Delta m = 1$ through the transfer of the spin angular momentum. The additional unit of orbital angular momentum— $\boldsymbol{k}_\gamma \times \boldsymbol{r}_e = \hbar$ —is oriented perpendicularly to the quantization axis. It increases the magnitude of the electron angular momentum but has no effect on its projection m onto $\hat{\boldsymbol{k}}_\gamma$. The strong resemblances between the measured angular emission patterns and $|Y_{21}|^2$, as demonstrated in Figures 2C,F, underline that QFM electrons originate from a pure quadrupole contribution to photoionization. Note that this agreement is better for He, and we suspect this is simply

due to larger momentum uncertainty in case of H_2. In our experiment, one of the two QFM electron momentum vectors is reconstructed by means of momentum conservation. This is less accurate for H_2 because the ions' center-of-mass momentum has to be retrieved from two protons instead of being measured via the doubly charged nucleus. Thus, the momentum uncertainty propagating to the calculated electron is larger in the case of H_2 than for He (see Refs. [15,19] for further details). While such a four-fold symmetry in the angular emission pattern of QFM electrons has already been shown for He PDI at 1100 eV photon energy [18], the results shown in Figure 2C for H_2 PDI further support our current understanding of quasifree photoionization.

3.2. Transfer of Photon Momentum

Nondipolar photoionization induces a forward-backward asymmetry in light propagation direction into the momentum distributions of the reaction fragments. This is due to the nonzero linear photon momentum k_γ and the interference between electric dipole and higher multipole contributions to the photoionization process. The question of which fragments obtain the photon momentum after the reaction has been investigated since the early days of photoionization studies [31,32]. In the case of photo-single-ionization, momentum and energy conservation dictate that the center of mass—which is essentially the residual photo-ion—obtains the photon momentum [21]. Additional degrees of freedom allow for a more intricate sharing of the photon momentum between the reaction fragments in photo-double ionization. However, a recent experiment–theory collaboration investigated He PDI up to 1100 eV photon energy and showed that the momentum distribution of helium nuclei after double ionization exhibits the same forward-backward asymmetry as helium nuclei from single ionization [29]. In this photon–energy range, He PDI is dominated by the shake-off process while the quasifree mechanism is negligible in absolute terms. Apparently, the shake-off process, where the second electron is emitted due to electron–electron correlation [33,34], treats the photon momentum similarly to how single ionization does, and the photon momentum is imparted onto the doubly charged helium nucleus. However, the quasifree mechanism proceeds without involvement of the nucleus, as the photon couples directly to the two electrons. Hence, one could expect that the photon momentum is not imprinted onto the photo-ion.

In order to test this assumption, we inspect the momentum distributions of photo-ions after He PDI at 800 eV photon energy in Figure 3 for SO (A) and QFM (B) by selecting subsets of our data.

In panel A, the measured photo-ion momenta accumulate on a semicircle with a radius that equals the maximum electron momentum and which is off-centered to the right by the magnitude of the photon momentum ($k_\gamma = 0.215$ au), indicating the transfer of the photon momentum onto the photo-ion. Note that this is the same behavior that has previously been shown for He single ionization [35]. In panel B, however, the measured average momentum of QFM photo-ions in light propagation direction is much closer to zero. This is even more apparent in panel C, where we projected the distribution shown in panel B onto the light propagation direction and determined the center through a Gaussian fit (solid blue line). Our experimental results speak in favor of the assumption that QFM photo-ions do not receive the photon momentum in the double-ionization process.

Further proof are the results of nondipole TDSE calculations for He double ionization at 800 eV photon energy, and linearly polarized light that are shown in Figure 3D. The local maximum of the nondipole curve (red line) that corresponds to QFM is exactly at zero, while the outer local maxima are shifted to the right by the magnitude of the photon momentum.
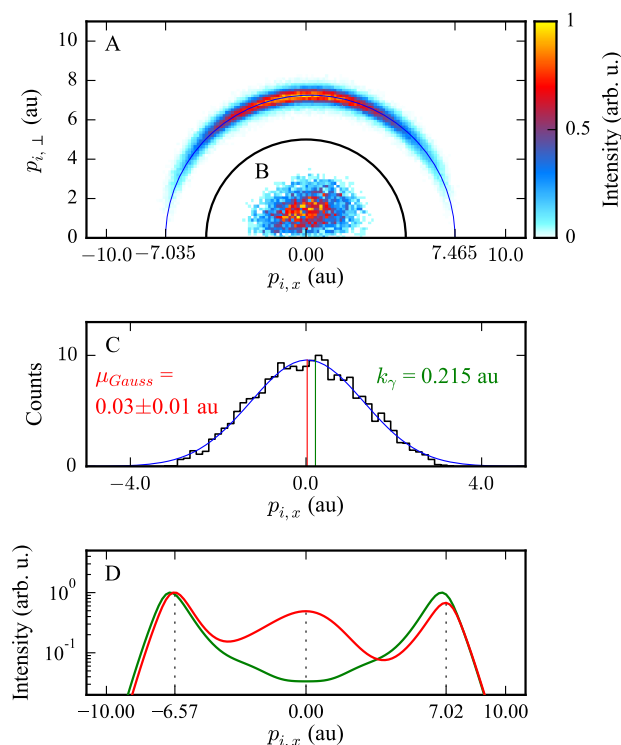
Figure 3. Photo-ion distributions of He double ionization by a single 800 eV photon. (**A**) The experimental data shown are limited to $\varepsilon < 0.005$ or $\varepsilon > 0.995$ and correspond to double ionization through the shake-off process. The blue semicircle is shifted to the right by the photon momentum. The SO photo-ions accumulate on this semicircle. (**B**) The experimental data shown are limited to $0.35 < \varepsilon < 0.65$ and $\vartheta_{12} > 160°$. They resemble double ionization via QFM. (**C**) Projection of data from B onto the *x* axis (black) and Gaussian fit (blue) to obtain the center of the momentum distribution of QFM photo-ions along the light propagation direction (red, μ_{Gauss}). Note that the indicated error is the standard deviation of the mean value from the Gaussian fit estimated as the square root of the respective diagonal element of the covariance matrix. The green line indicates the photon momentum for comparison. (**D**) Dipole (green) and nondipole (red) TDSE calculations for helium double ionization with 800 eV linearly polarized photons. The polarization vector is parallel to the *z* axis and the data shown are limited to $p_{i,y} = 0 \pm \frac{p_{\text{single}}}{2}$ & $p_{i,z} = 0 \pm \frac{p_{\text{single}}}{4}$. Experiment and theory suggest that the photon momentum is not imprinted onto QFM photo-ions.

4. Conclusions

We have investigated the quasifree mechanism of one-photon double ionization of He and H_2 at 800 eV photon energy and addressed two open questions concerning this intriguing process. We found the four-fold symmetry in the angular emission pattern of QFM electrons from H_2 double ionization that underlines the quadrupole nature of the process. Furthermore, we showed that the photon momentum is not transferred onto the photo-ion in quasifree photoionization, which is in contrast to single ionization in general and double ionization by means of electron–electron correlation.

Author Contributions: Conceptualization, M.S.S.; Experimental preapration, S.G., F.T., T.J. and M.S.S.; Experiment performed, S.G., F.T., K.F., N.S., A.P., L.K., M.K., T.J. and M.S.S.; Data analysis, S.G.; Validation, F.T., T.J., R.D. and M.S.S.; Supervision, T.J., R.D. and M.S.S.; Theory calculations, Y.-K.F. and L.-Y.P.; Writing—original draft preparation, S.G.; Writing—review and editing, S.G., F.T., Y.-K.F., K.F., N.S., A.P., L.K., M.K., L.-Y.P., T.J., R.D. and M.S.S.; Visualization, S.G.; Funding acquisition, T.J., R.D. and M.S.S. All authors have read and agreed to the published version of the manuscript.

References

1. Amusia, M.Y.; Drukarev, E.G.; Gorshkov, V.G.; Kazachkov, M.O. Two-electron photoionization of helium. *J. Phys. B* **1975**, *8*, 1248. [CrossRef]
2. Amusia, M.Y.; Drukarev, E.G.; Liverts, E.Z. Small recoil momenta double ionization of He and two-electron ions by high energy photons. *Eur. Phys. J. D* **2020**, *74*, 173. [CrossRef]
3. Amusia, M.Y.; Drukarev, E.G.; Liverts, E.Z.; Mikhailov, A.I. Effects of small recoil momenta in one-photon two-electron ionization. *Phys. Rev. A* **2013**, *87*, 043423. [CrossRef]
4. Maulbetsch, F.; Briggs, J.S. Selection rules for transitions to two-electron continuum states. *J. Phys. B* **1995**, *28*, 551. [CrossRef]
5. Suric, T.; Drukarev, E.G.; Pratt, R.H. Characterization of high-energy photoionization in terms of the singularities of the atomic potential. I. Photoionization of the ground state of a two-electron atom. *Phys. Rev. A* **2003**, *67*, 022709. [CrossRef]
6. Amusia, M.Y.; Drukarev, E.G.; Mandelzweig, V.B. Quasifree Mechanism in Ionization Processes. *Phys. Scr.* **2005**, *72*, C22. [CrossRef]
7. Drukarev, E.G. Breakdown of asymptotics of the double photoionization of helium at the high-energy limit. *Phys. Rev. A* **1995**, *51*, R2684. [CrossRef]
8. Schöffler, M.S.; Stuck, C.; Waitz, M.; Trinter, F.; Jahnke, T.; Lenz, U.; Jones, M.; Belkacem, A.; Landers, A.L.; Pindzola, M.S.; et al. Ejection of Quasi-Free-Electron Pairs from the Helium-Atom Ground State by Single-Photon Absorption. *Phys. Rev. Lett.* **2013**, *111*, 013003. [CrossRef]
9. Spielberger, L.; Jagutzki, O.; Dörner, R.; Ullrich, J.; Meyer, U.; Mergel, V.; Unverzagt, M.; Damrau, M.; Vogt, T.; Ali, I.; et al. Separation of Photoabsorption and Compton Scattering Contributions to He Single and Double Ionization. *Phys. Rev. Lett.* **1995**, *74*, 4615. [CrossRef]
10. Spielberger, L.; Jagutzki, O.; Krässig, B.; Meyer, U.; Khayyat, K.; Mergel, V.; Tschentscher, T.; Buslaps, T.; Bräuning, H.; Dörner, R.; et al. Double and Single Ionization of Helium by 58-keV X Rays. *Phys. Rev. Lett.* **1996**, *76*, 4685. [CrossRef]
11. Kircher, M.; Trinter, F.; Grundmann, S.; Kastirke, G.; Weller, M.; Vela-Perez, I.; Khan, A.; Janke, C.; Waitz, M.; Zeller, S.; et al. Ion and Electron Momentum Distributions from Single and Double Ionization of Helium Induced by Compton Scattering. *Phys. Rev. Lett.* **2022**, *128*, 053001. [CrossRef] [PubMed]
12. Smeenk, C.T.L.; Arissian, L.; Zhou, B.; Mysyrowicz, A.; Villeneuve, D.M.; Staudte, A.; Corkum, P.B. Partitioning of the Linear Photon Momentum in Multiphoton Ionization. *Phys. Rev. Lett.* **2011**, *106*, 193002. [CrossRef] [PubMed]
13. Chelkowski, S.; Bandrauk, A.D.; Corkum, P.B. Photon Momentum Sharing between an Electron and an Ion in Photoionization: From One-Photon (Photoelectric Effect) to Multiphoton Absorption. *Phys. Rev. Lett.* **2014**, *113*, 263005. [CrossRef] [PubMed]
14. Hartung, A.; Eckart, S.; Brennecke, S.; Rist, J.; Trabert, D.; Fehre, K.; Richter, M.; Sann, H.; Zeller, S.; Henrichs, K.; et al. Magnetic fields alter strong-field ionization. *Nat. Phys.* **2019**, *15*, 1222–1226. [CrossRef]
15. Grundmann, S.; Trabert, D.; Fehre, K.; Strenger, N.; Pier, A.; Kaiser, L.; Kircher, M.; Weller, M.; Eckart, S.; Schmidt, L.P.H.; et al. Zeptosecond birth time delay in molecular photoionization. *Science* **2020**, *370*, 339–341. [CrossRef]
16. Hartung, A.; Brennecke, S.; Lin, K.; Trabert, D.; Fehre, K.; Rist, J.; Schöffler, M.S.; Jahnke, T.; Schmidt, L.P.H.; Kunitski, M.; et al. Electric Nondipole Effect in Strong-Field Ionization. *Phys. Rev. Lett.* **2021**, *126*, 053202. [CrossRef]
17. Lin, K.; Eckart, S.; Hartung, A.; Trabert, D.; Fehre, K.; Rist, J.; Schmidt, L.P.H.; Schöffler, M.S.; Jahnke, T.; Kunitski, M.; et al. Photoelectron energy peaks shift against the radiation pressure in strong-field ionization. *Sci. Adv.* **2022**, *8*, eabn7386. [CrossRef]
18. Grundmann, S.; Trinter, F.; Bray, A.W.; Eckart, S.; Rist, J.; Kastirke, G.; Metz, D.; Klumpp, S.; Viefhaus, J.; Schmidt, L.P.H.; et al. Separating Dipole and Quadrupole Contributions to Single-Photon Double Ionization. *Phys. Rev. Lett.* **2018**, *121*, 173003. [CrossRef]
19. Grundmann, S.; Serov, V.V.; Trinter, F.; Fehre, K.; Strenger, N.; Pier, A.; Kircher, M.; Trabert, D.; Weller, M.; Rist, J.; et al. Revealing the two-electron cusp in the ground states of He and H_2 via quasifree double photoionization. *Phys. Rev. Res.* **2020**, *2*, 033080. [CrossRef]
20. Viefhaus, J.; Scholz, F.; Deinert, S.; Glaser, L.; Ilchen, M.; Seltmann, J.; Walter, P.; Siewert, F. The Variable Polarization XUV Beamline P04 at PETRA III: Optics, mechanics and their performance. *Nucl. Instrum. Methods Phys. Res. A* **2013**, *710*, 151. [CrossRef]

21. Dörner, R.; Mergel, V.; Jagutzki, O.; Spielberger, L.; Ullrich, J.; Moshammer, R.; Schmidt-Böcking, H. Cold Target Recoil Ion Momentum Spectroscopy: A 'momentum microscope' to view atomic collision dynamics. *Phys. Rep.* **2000**, *330*, 95–192. [CrossRef]

22. Ullrich, J.; Moshammer, R.; Dorn, A.; Dörner, R.; Schmidt, L.P.H.; Schmidt-Böcking, H. Recoil-ion and electron momentum spectroscopy: Reaction-microscopes. *Rep. Prog. Phys.* **2003**, *66*, 1463. [CrossRef]

23. Jahnke, T.; Foucar, L.; Titze, J.; Wallauer, R.; Osipov, T.; Benis, E.P.; Alnaser, A.; Jagutzki, O.; Arnold, W.; Semenov, S.K.; et al. Vibrationally Resolved K-shell Photoionization of CO with Circularly Polarized Light. *Phys. Rev. Lett.* **2004**, *93*, 083002. [CrossRef]

24. Jagutzki, O.; Mergel, V.; Ullmann-Pfleger, K.; Spielberger, L.; Spillmann, U.; Dörner, R.; Schmidt-Böcking, H. A broad-application microchannel-plate detector system for advanced particle or photon detection tasks: Large area imaging, precise multi-hit timing information and high detection rate. *Nucl. Instrum. Methods Phys. Res. A* **2002**, *477*, 244–249. [CrossRef]

25. Jagutzki, O.; Lapington, J.S.; Worth, L.B.C.; Spillman, U.; Mergel, V.; Schmidt-Böcking, H. Position sensitive anodes for MCP read-out using induced charge measurement. *Nucl. Instrum. Methods Phys. Res. A* **2002**, *477*, 256–261. [CrossRef]

26. Zhang, Z.; Peng, L.-Y.; Xu, M.-H.; Starace, A.F.; Morishita, T.; Gong, Q. Two-photon double ionization of helium: Evolution of the joint angular distribution with photon energy and two-electron energy sharing. *Phys. Rev. A* **2011**, *84*, 043409. [CrossRef]

27. Jiang, W.-C.; Peng, L.-Y.; Xiong, W.-H.; Gong, Q. Comparison study of electron correlation in one-photon and two-photon double ionization of helium. *Phys. Rev. A* **2013**, *88*, 023410. [CrossRef]

28. Jiang, W.-C.; Shan, J.-Y.; Gong, Q.; Peng, L.-Y. Virtual Sequential Picture for Nonsequential Two-Photon Double Ionization of Helium. *Phys. Rev. Lett.* **2015**, *115*, 153002. [CrossRef]

29. Chen, S.-G.; Jiang, W.-C.; Grundmann, S.; Trinter, F.; Schöffler, M.S.; Jahnke, T.; Dörner, R.; Liang, H.; Wang, M.-X.; Peng, L.-Y.; et al. Photon Momentum Transfer in Single-Photon Double Ionization of Helium. *Phys. Rev. Lett.* **2020**, *124*, 043201. [CrossRef]

30. Weber, T.; Czasch, A.; Jagutzki, O.; Müller, A.; Mergel, V.; Kheifets, A.; Feagin, J.; Rotenberg, E.; Meigs, G.; Prior, M.H.; et al. Fully Differential Cross Sections for Photo-Double-Ionization of D_2. *Phys. Rev. Lett.* **2004**, *92*, 163001. [CrossRef]

31. Auger, P. Etude expérimentale des directions d'émission des photoélectrons. *J. Phys. Radium* **1927**, *8*, 85–92. [CrossRef]

32. Sommerfeld, A.; Schur, G. Über den Photoeffekt in der K-Schale der Atome, insbesondere über die Voreilung der Photoelektronen. *Ann. Phys.* **1930**, *396*, 409–432. [CrossRef]

33. Briggs, J.S.; Schmidt, V. Differential cross sections for photo-double-ionization of the helium atom. *J. Phys. B* **2000**, *33*, R1. [CrossRef]

34. Kheifets, A. On different mechanisms of the two-electron atomic photoionization. *J. Phys. B* **2001**, *34*, L247. [CrossRef]

35. Grundmann, S.; Kircher, M.; Vela-Perez, I.; Nalin, G.; Trabert, D.; Anders, N.; Melzer, N.; Rist, J.; Pier, A.; Strenger, N.; et al. Observation of Photoion Backward Emission in Photoionization of He and N_2. *Phys. Rev. Lett.* **2020**, *124*, 233201. [CrossRef]